# Functionalizing Carbon Substrates with a Covalently Attached Cobalt Redox Buffer for Calibration-Free Solid-Contact Ion-Selective Electrodes

Minog Kim,[†] Xin I. N. Dong,[†] Brian D. Spindler, Philippe Bühlmann,[*] and Andreas Stein[*]

Department of Chemistry, University of Minnesota, 207 Pleasant Street SE, Minneapolis, MN 55455-0431, USA

*Corresponding authors E-mail: a-stein@umn.edu, buhlmann@umn.edu

[†]These authors contributed equally.

**ABSTRACT**

With a view to potentiometric sensing with minimal calibration requirements and high long-term stability, colloid-imprinted mesoporous (CIM) carbon was functionalized by covalent attachment of a cobalt redox buffer and used as a new solid contact for ion-selective electrodes (ISEs). The CIM carbon surface was first modified by electroless grafting of a terpyridine ligand (Tpy-ph-) using diazonium chemistry, followed by stepwise binding of Co(II) and an additional Tpy ligand to the grafted ligand, forming a bis(terpyridine) Co(II) complex, CIM-ph-Tpy-Co(II)-Tpy. Half a molar equivalent of ferrocenium tetrakis(3-chlorophenyl)borate was then used to partially oxidize the Co(II) complex. Electrodes prepared with this surface-attached CIM-ph-Tpy-Co(III/II)-Tpy redox buffer as solid contact were tested as $K^+$ sensors in combination with valinomycin as ionophore and Dow 3140 silicone or plasticized poly(vinyl chloride) (PVC) as matrixes for the ion-selective membrane (ISM). This solid contact is characterized by a redox capacitance of 3.26 F/g, ensuring a well-defined interfacial potential that underpins the transduction mechanism. By use of a redox couple as internal reference element to control the phase boundary potential at the interface of the ISM and the CIM carbon solid contact, solid-contact ion-selective electrodes (SC-ISEs) with a standard deviation of $E°$ as low as 0.3 mV for plasticized PVC and 3.5 mV for Dow 3140 silicone ISMs were obtained. Over 100 h, these SC-ISEs exhibit an EMF drift of 20 μV/h for plasticized PVC and 62 μV/h for silicone ISMs. The differences in long-term stability and reproducibility between electrodes with ISMs comprising either a plasticized PVC or silicone matrix offer valuable insights into the effect of the polymeric matrix on sensor performance.

Keywords: Redox buffer, ion-selective electrode, calibration-free sensor, sensor miniaturization, solid contact

## INTRODUCTION

Ion-selective electrodes (ISEs) are widely utilized in clinical analysis, process control, and environmental analysis.[1-5] Because conventional ISEs with an inner filling solution are difficult to miniaturize, they are not readily amenable to mass manufacturing and cannot be easily integrated into wearable and implantable devices.[6] Therefore, solid-contact ISEs (SC-ISEs) have attracted much interest.[7-17] While early SC-ISEs had the ion-selective membrane (ISM) directly applied onto a metal contact,[18] this did not result in a well-defined interfacial potential between the ISM and the underlying electron conductor, and it led to water layer formation. Consequently, these electrodes had poor stabilities and poor electrode-to-electrode reproducibilities of the standard potential, $E°$, of the electrochemical cell, as measured with a target ion activity of 1 in the sample.[19]

To stabilize this interfacial potential, intermediate layers consisting of conducting polymers with a high redox capacitance were introduced.[7-9, 17] The $E°$ values of such are, however, not very reproducible, and they change over time, which can be attributed to a wide variability in local conformations as well as spontaneous oxidation by ambient oxygen.[10, 20, 21] In an attempt to use a more well-defined molecular redox buffer, redox-active self-assembled monolayers (SAMs) were explored, such as ferrocene-modified SAMs, but the redox buffer capacity of those sensors was insufficient due to the small amount of redox species in a monolayer on a planar substrate.[22, 23] More recently, this concept has been extended to polymers doped with metal–organic complexes[24-27] and TEMPO[17, 28] as redox-active species, and the advantages of using redox buffers comprising both the reduced and oxidized forms of the redox buffer have been shown.[29-32]

As an alternate approach, ISEs with high surface area carbons have been used.[33-37] The large surface areas result in a high capacitance of the interface between the ISM and the solid contact and, consequently, the corresponding interfacial phase boundary potential is highly resistant to

change, which minimizes long-term drift.[36, 38] In particular, in our previous work, ISEs with colloid-imprinted mesoporous (CIM) carbon as solid contact exhibited $E°$ values with a standard deviation of 7.3 mV and a potential drift of only 1.3 μV/h over 70 h.[37] Combining a high surface area carbon solid contact with doping of the ISM membrane with a hydrophobic Co(III/II) redox buffer, the standard deviation of $E°$ could be further reduced to 0.7 mV.[37] However, loss of redox buffer from the ISM into the aqueous sample solution was observed, which is not acceptable for long term measurement.[29, 30]

Here, we introduce CIM carbon with a covalently attached redox buffer (CIM-ph-Tpy-Co(III/II)-Tpy) as a novel solid-contact material for the fabrication of ion-selective electrodes with minimal calibration requirements. The combined use of a high solid-contact surface area, as provided by the mesoporous carbon, and the attachment of the redox buffer to the carbon surface throughout the entire solid-contact layer result in a highly reproducible standard potential ($E°$). It also avoids leaching of the redox buffer from the ISM into the aqueous sample solution. Results for SC-ISEs both with plasticized PVC and silicone based ISMs are presented.

## EXPERIMENTAL SECTION

**Reagents and Materials.** Reagents were obtained from the following sources: 4-([2,2':6',2''-terpyridin]-4'-yl)aniline (Tpy-ph-$NH_2$, 97%) from Ambeed (Arlington Heights, IL, USA); 2,2':6',2''-terpyridine (Tpy, 98%), polytetrafluoroethylene preparation (60 wt % Teflon dispersion in $H_2O$) from Sigma-Aldrich (St. Louis, MO, USA); mesophase pitch from Mitsubishi Gas Chemicals (Tokyo, Japan). The Supporting Information describes the experimental details for the preparation of ferrocenium tetrakis(3-chlorophenyl)borate (from ferrocenium tetrafluoroborate and ammonium tetrakis(3-chlorophenyl)-borate), colloid-imprinted mesoporous (CIM) carbon,

and Co(III/II) redox buffer-functionalized CIM carbon (CIM-ph-Tpy-Co(III/II)-Tpy). For other reagents, see the Supporting Information.

**Electrode Fabrication.** ISEs with silicone-based sensing membranes were prepared following a previously reported procedure.[39] A graphite rod (outer diameter 0.235 mm) was inserted into a glass tube (inner diameter 0.235 mm) and the gap between the graphite and the tube was filled with aqueous 60 wt % polytetrafluoroethylene dispersion, followed by drying at room temperature overnight. The graphite surface exposed at the end of the tube was then polished with sandpaper (starting with 300 and finishing with 1500 grit) and rinsed first with water and then ethanol, followed by drying with a stream of argon. Functionalized CIM carbon films were made by mixing 100 mg of functionalized CIM carbon powder with 0.1 mL of the 5 wt % polytetrafluoroethylene dispersion, followed by roller pressing of this blend to a thickness of 120 μm. Disks were then cut out of the functionalized CIM carbon film (diameter of 5.6 mm, ≈ 5 mg) using a hole punch and placed on top of the graphite rod, followed by application of 50 μL of toluene onto the functionalized CIM carbon film and the exposed end of the glass tube, avoiding bubble formation on the functionalized CIM carbon in the subsequent step. Then, a total of 200 μL of the ISM solution was added onto the functionalized CIM carbon film, and the ISM was cured in an oven at 55 °C for 24 h. ISM solutions for valinomycin-doped $K^+$ Dow 3140 ISMs were prepared by dissolving in 1 mL of freshly distilled toluene 200 mg of Dow 3140, 2.0 mg of valinomycin as ionophore, and 0.4 mg of ammonium tetrakis(3-chlorophenyl)borate (50 mol % with respect to the ionophore) to provide ionic sites. The advantage of using a glass tube for the preparation of these electrodes is that the silicone ISMs are covalently attached to the electrode bodies by formation of Si–O–Si bonds.

ISMs with a plasticized PVC matrix were prepared by dissolving in 1 mL of freshly distilled THF the ISM ingredients: 66 mg of PVC as the polymer matrix, 132 mg of bis(2-ethylhexyl) sebacate (DOS) as plasticizer, 2.0 mg of valinomycin as ionophore, and 0.4 mg of ammonium tetrakis(3-chlorophenyl)borate (50 mol % with respect to the ionophore) to provide ionic sites. Functionalized CIM carbon powder was sonicated in dry THF for 20 min to produce a 50 mg/mL suspension, and then 40 μL of this suspension was drop cast onto a glassy carbon electrode (a glassy carbon rod encased into an inert polymer; CH Instruments, Austin, TX, USA), forming CIM carbon films as ISE solid-contact layers with a thickness of approximately 200 μm and a weight of 2 mg. To form plasticized ISMs with a thickness of approximately 100 μm, two portions of the above PVC membrane solution (20 μL, followed by 30 μL) were drop cast onto the functionalized CIM carbon layer on a glassy carbon disk CHI electrode and allowed to dry overnight. As a precaution to avoid the possible delamination of the ISMs and functionalized CIM carbon films from the glassy carbon electrodes and to make sure that there was a good contact between the different layers of the electrode/CIM carbon/ISM construct, the coated electrodes were mounted into cylindrical bodies with an o-ring in between the electrode body and the ISM. The outer diameter of the o-ring was chosen to match the inner diameter of the electrode body.

**Potentiometric Measurements.** Potentiometric measurements were performed with an EMF 16-channel potentiometer (Lawson Labs, Malvern, PA, USA) controlled by 1.03 EMF Suite software (Fluorous Innovation, Arden Hills, MN, USA). A double-junction reference electrode (DX200, Mettler Toledo, Switzerland; AgCl-saturated 3.0 M KCl as inner reference electrolyte and 1.0 M LiOAc as bridge electrolyte) was used as a conventional external reference electrode for calibration experiments, and a Ag/AgCl wire was used as a reference electrode for long-term stability experiments in 1 mM KCl samples in a temperature-controlled chamber at 25 ˚C. All

electrodes were conditioned in a 1 mM KCl solution for at least 24 h to ensure full conditioning before measurements. All emf values were corrected for the liquid junction potential at the double-junction reference electrode by using the Henderson equation.[40] Activity coefficients were calculated based on a two-parameter Debye-Hückel approximation.[41]

## RESULTS AND DISCUSSION

**CIM Carbon.** The goal of this work was to covalently introduce a molecular high-capacity redox buffer to the interface between the ion-selective membrane and an underlying solid contact with a high surface area. A planar substrate with a small surface area would not give a sufficiently large buffer capacity.[7,15] Therefore, we used in this work CIM carbon as the substrate onto which the redox buffer was grafted. CIM carbon is a porous carbon with uniformly sized, interconnected, but disordered spherical mesopores and a high surface area. After thermal reduction in hydrogen, it has a low content of oxygen on the surface, which provides a hydrophobic environment and prevents water layer formation at the interface between the ISM and solid contact.[10, 42] $N_2$ physisorption analysis of CIM carbon showed a typical type IV isotherm (Figure S1), from which a DFT surface area of 373 $m^2/g$ was calculated (Table S1). The thus determined pore sizes are in the 20–30 nm range, in agreement with the dimensions of the pores as observed by scanning electron microscopy (SEM, see Figure 1).

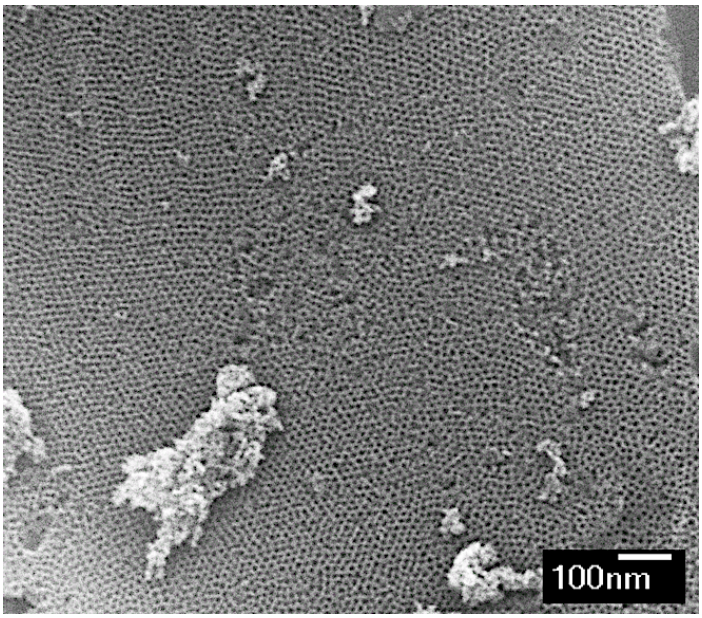


**Figure 1.** SEM image of a CIM carbon particle, showing the mesopores on its surface. Reprinted with permission from Dong et al., *ACS Sens.* **2023**, *8*, 1774. Copyright 2023, American Chemical Society.

**Cobalt Redox Buffer-Functionalized CIM Carbon.** The synthetic approach to prepare the redox buffer CIM-ph-Tpy-Co(III/II)-Tpy, as shown in Scheme 1, consisted of the synthesis of a diazonium derivative of terpyridine (Tpy-ph-$N_2^+$), grafting of this ligand by covalent bond formation to the CIM carbon substrate, complexation of Co(II) to the surface-attached terpyridine ligands, and completion of the octahedral Co(II) complex by reaction with a second terpyridine ligand. This was followed by partial oxidation of CIM-ph-Tpy-Co(II)-Tpy to CIM-ph-Tpy-Co(III)-Tpy.

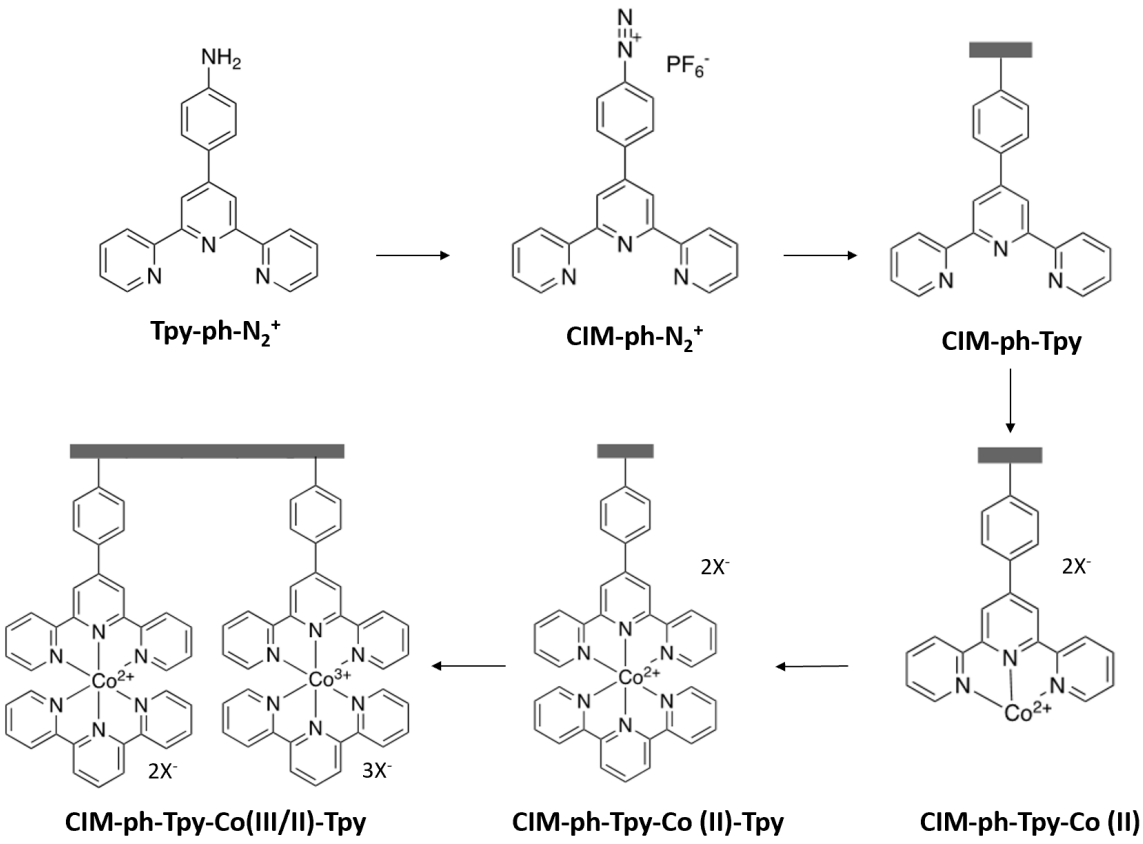


**Scheme 1.** Schematic of the functionalization of CIM carbon with ph-Tpy-Co(III/II)-Tpy. $X^-$ refers to the counter ion.

The first terpyridine ligand was covalently attached to the CIM carbon by electroless grafting using the diazonium compound Tpy-ph-$N_2^+$ (for experimental details, see the Supporting Information). Diazonium salts are easily reduced while releasing $N_2$, leading to aryl radicals that readily bind to carbon surfaces and various metal oxides.[43, 44] Similar grafting of Tpy-ph-$N_2^+$ has been performed previously on various substrates, such as glassy carbon,[45] carbon black,[46] multiwalled carbon nanotubes,[47-50] indium-tin oxide,[51] metal oxide thin films deposited on fluorine-doped tin oxide glass,[52] and others. In this work, the $PF_6^-$ salt of Tpy-ph-$N_2^+$ was prepared

by diazotization of the corresponding amine, followed by precipitation with $KPF_6$. $^1H$ NMR, mass and IR spectra confirm the purity of the Tpy-ph-$N_2^+$ product (see Figures S2–S4).

For electroless grafting of the terpyridine ligand onto the CIM carbon powder, the amount of Tpy-ph ligand attached to the CIM carbon after 3 h exposure of the CIM carbon to Tpy-ph-$N_2^+$ was determined by comparison of the experimental weight ratio of carbon and nitrogen in the functionalized CIM carbon (from combustion analysis) to the corresponding C:N ratio as expected from the surface area of the carbon, assuming that a complete monolayer is formed over the entire CIM carbon surface area. The C:N ratio expected for full monolayer coverage was calculated based on the ligand size (footprint of bis(terpyridine) = $1.21\times10^{-18}$ $m^2$) and the DFT surface area of the CIM carbon (373 $m^2/g$), with the assumptions (i) that the ligand complexes are perpendicularly packed on the carbon surface and (ii) that the complexes cover all of the DFT surface area (as shown in Figure S5). Based on these estimates, electroless grafting of 10 mg CIM carbon with 50 mM Tpy-ph-$N_2^+$ in 2 mL DMSO (twentyfold excess with respect to expected monolayer coverage) resulted in a surface concentration of the redox buffer corresponding to 66% of a full monolayer over the entire carbon surface. In contrast, when 1 g CIM carbon was reacted with 10 mL of a 50 mM solution of Tpy-ph-$N_2^+$ in DMSO (which corresponds to only one equivalent of a theoretical monolayer), the estimated monolayer coverage reached only 20% (for details, see the Supporting Information). The latter modified CIM carbon was used after complete functionalization for subsequent potentiometric experiments.

The CIM carbon with the covalently attached Tpy-ph ligand was further modified by allowing Co(II) to bind to the Tpy groups to form CIM-ph-Tpy-Co(II). This was achieved by exposure of the CIM-ph-Tpy powder for 24 h to an ethanolic solution (10 mM, 10 mL) that contained 1 equivalent of $CoCl_2\cdot6H_2O$ with respect to the attached ligand, Tpy-ph. Upon isolation of the

modified CIM carbon by centrifugation, the resulting powder was reacted with 10 mL of 10 mM terpyridine ethanolic solution (1 equivalent relative to CIM-ph-Tpy-Co(II)) for 3 h, followed by isolation of the desired CIM-ph-Tpy-Co(II)-Tpy powder. Analysis by inductively-coupled plasma–optical emission spectrometry (ICP-OES) showed that the thus obtained CIM-ph-Tpy-Co(II)-Tpy contained 0.387 wt % cobalt (corresponding to 0.079 atom %). This amount of cobalt corresponds to a 13% monolayer coverage.

In the final synthesis step, the thus obtained CIM-ph-Tpy-Co(II)-Tpy was partially oxidized by exposure to a solution of ferrocenium tetrakis(3-chlorophenyl)borate in cyclohexane. The total amount of the ferrocenium was chosen to be sufficient to convert half of the Co(II) to Co(III), producing a Co(III/II) redox buffer with a 1:1 mixture of Co(III) and Co(II). We chose ferrocenium as the oxidizing reagent because the reaction of Co(II) with ferrocenium gives ferrocene, an electrically neutral species that does not interfere with any ion equilibria and does not affect the emf.[31] Therefore, any residual ferrocene left in an ion-selective membrane by the time the ISE is being used does not affect the sensor's performance. Moreover, due to its limited lipophilicity, distribution of any remaining ferrocene into the conditioning solution is expected, and oxidation of ferrocene in the aqueous environment by ambient oxygen to the more hydrophilic ferrocenium provides a thermodynamic sink that would further enhance the transfer of ferrocene out of the sensing membranes. Tetrakis(3-chlorophenyl)borate was chosen as the counter ion of the electrically charged ferrocenium reagent because, after the redox reaction, this anion remains associated with the surface-bound Co(III/II) complexes. Because tetrakis(3-chlorophenyl)borate is also the ionic site used to control the potentiometric selectivity of all sensing membranes described in this work, use of the ferrocenium tetrakis(3-chlorophenyl)borate as oxidizing reagent also avoids any subsequent ion exchange with samples.

We wish to emphasize that the selection of this particular oxidizing reagent is quite critical to a good performance of the final SC-ISEs. Specifically, we previously used elemental bromine, $Br_2$, to successfully oxidize Co(II)complexes for use in redox buffers.[29, 30] However, the use of an excess of bromine can be problematic due to its high reactivity. Moreover, when we used in preliminary experiments bromine as the oxidizing reagent for surface-bound Co(II), the resulting surface-bound Co(III) complexes were associated with bromide as counterions, which for reasons of electroneutrality cannot be removed by washing with a solvent. When a sensing membrane was subsequently applied onto a carbon surface modified this way, persistent emf drifts were observed. A possible explanation for this observation may be the presence of bromide at the interface of the sensing membrane and the CIM carbon, which may enter the ISM by ion exchange with ionic sites and, subsequently, with anions in samples, giving rise to transmembrane ion fluxes.

We conclude that the electroless fabrication of CIM-ph-Tpy-Co(II)-Tpy using ferrocenium tetrakis(3-chlorophenyl)borate, as described above, is likely the most convenient method for the fabrication of large numbers of sensors, such as in mass manufacturing. However, we note that CIM-ph-Tpy-Co(II)-Tpy can also be prepared by electrochemical grafting of Tpy-ph-$N_2^+$ onto a glassy carbon electrode (see the Supporting Information).

**Cyclic Voltammetry (CV) of the Surface-Attached Tpy-Co(III/II)-Tpy-ph.** Because of the mesoporous structure of CIM-ph-Tpy-Co(II)-Tpy, peaks for surface-bound redox-active species are difficult to assign in cyclic voltammograms with CIM carbon electrodes. Therefore, to confirm the formation of the surface-attached Tpy-Co(III/II)-Tpy-ph complexes, we also attached these complexes to planar glassy carbon electrodes (GCEs) rather than CIM carbon (for experimental details, see the Supporting Information).

GCE-ph-Tpy-Co(II) was prepared by electrochemically grafting the ph-Tpy ligand to GCEs, followed by soaking GCE-ph-Tpy in ethanolic $CoCl_2$ solution. Figure 2 shows the CV curve obtained in 0.1 M $TEABF_4$/MeCN with a $Ag/Ag^+$ reference and a Pt counter electrode within the potential range of –0.5 to +0.5 V vs. $Ag/Ag^+$. GCE-ph-Tpy-Co(II) did not show any prominent redox couple between –0.5 and +0.5 V, where the bis(terpyridine) complex Tpy-Co(III/II)-Tpy would appear, even when considering a possible slight shift in potential due to the different ligand environment (Tpy *vs.* Tpy-ph). This result implies that Co(II) was indeed incorporated in the functionalized GCE as a mono(terpyridine), that is, GCE-ph-Tpy-Co(II).

The GCE-ph-Tpy-Co(II) electrode was then immersed in 1 mM Tpy ethanolic solution for 3 h to attach Tpy as the capping ligand. The CV of GCE-ph-Tpy-Co(II)-Tpy shows a distinct Tpy-Co(III/II)-Tpy redox couple at –0.02 V (Figure 2). A surface coverage of $1.0\times10^{-11}$ mol was calculated by integrating the cathodic peak area from the CV curve. This value is close to the expected amount of Tpy-Co(III/II)-Tpy-ph in a monolayer on a planar GCE of this size ($9.7\times10^{-12}$ mol).

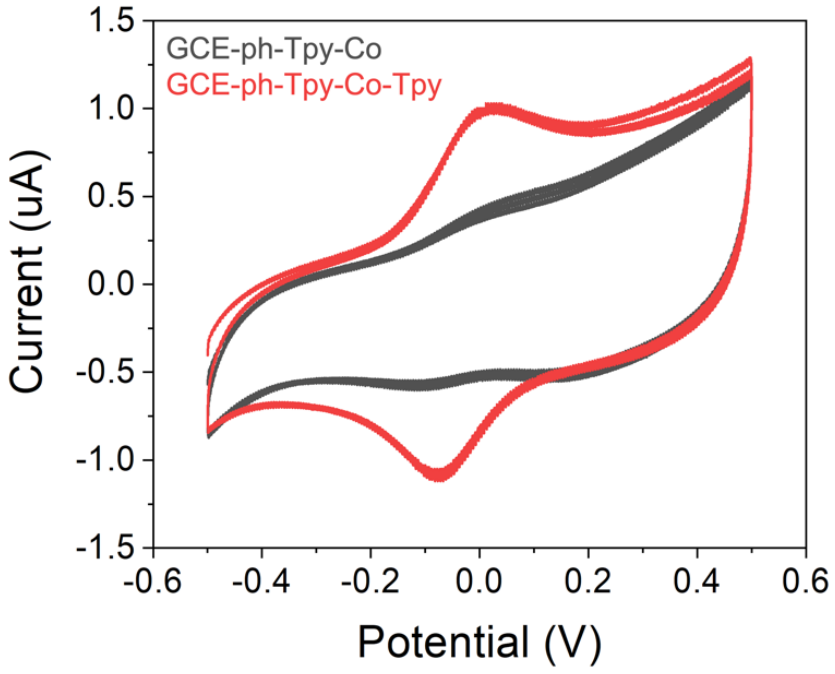

**Figure 2.** Cyclic voltammograms of the GCE-ph-Tpy-Co(II) and GCE-ph-Tpy-Co(II)-Tpy electrodes at 100 mV/s in acetonitrile. Shown are two full scan cycles for each electrode.

We note that the selection of the solvent for this voltammetric characterization is critical. Attempting the same type of experiment with dimethylformamide as solvent, we observed dissociation of the terpyridine ligand from GCE-ph-Tpy-Co(II)-Tpy during the approximately 20 min needed for degassing of the solution with argon (for further details, see the Supporting Information). To study this effect further, CVs were measured to monitor the intensity of the GCE-ph-Tpy-Co(III/II)-Tpy redox peaks after GCE-ph-Tpy-Co(II)-Tpy electrodes were exposed to several solvents for varying time periods (see Figure S11 and Table S2 of the Supporting Information). Exposures to DMF and acetonitrile resulted in a significant decrease after only 5 min, while complex dissociation was much slower in EtOH, $H_2O$, and 1,2-dichloroethane. All of these solvents have a rather high polarity, with dielectric constants >10. In cyclohexane, a solvent of low polarity with a dielectric constant of 2.0, the intensity of the GCE-ph-Tpy-Co(III/II)-Tpy peak did not decrease after 19 h, indicating greater stability of the complex in cyclohexane. We conclude that solvents of high polarity should be avoided in the fabrication and characterization of SC-ISEs comprising the surface-attached Tpy-Co(III/II)-Tpy-ph redox buffer. Indeed, the stability of the bis(terpyridine) complexes of Co(III) and Co(II) is one of the reasons why we chose to use for this work tridentate terpyridine ligands, rather than the bidentate ligands of earlier work with freely dissolved tris(phenanthrene) and tris(bipyridine) complexes of Co(III) and Co(II).[29, 30, 37]

**Potential Stability and Reproducibility of CIM-ph-Tpy-Co(III/II)-Tpy-Based SC-ISEs.** The cobalt redox buffer functionalized CIM carbon was used to prepare solid-contact ISEs comprising sensing membranes with valinomycin as $K^+$ ionophore and Dow 3140 as the polymeric membrane matrix. For comparison, three different electrode assemblies were used: (i) a graphite

rod coated directly with the ISM (graphite/ISM), (ii) a graphite rod coated with a non-functionalized CIM carbon intermediate layer and an ISM (graphite/CIM carbon/ISM), and (iii) a graphite rod coated with a cobalt redox buffer functionalized CIM carbon layer and an ISM (graphite/CIM-ph-Tpy-Co(III/II)-Tpy/ISM). The potentiometric $K^+$ calibration curves of these electrodes are shown in Figure 3 and summarized in Table 1.

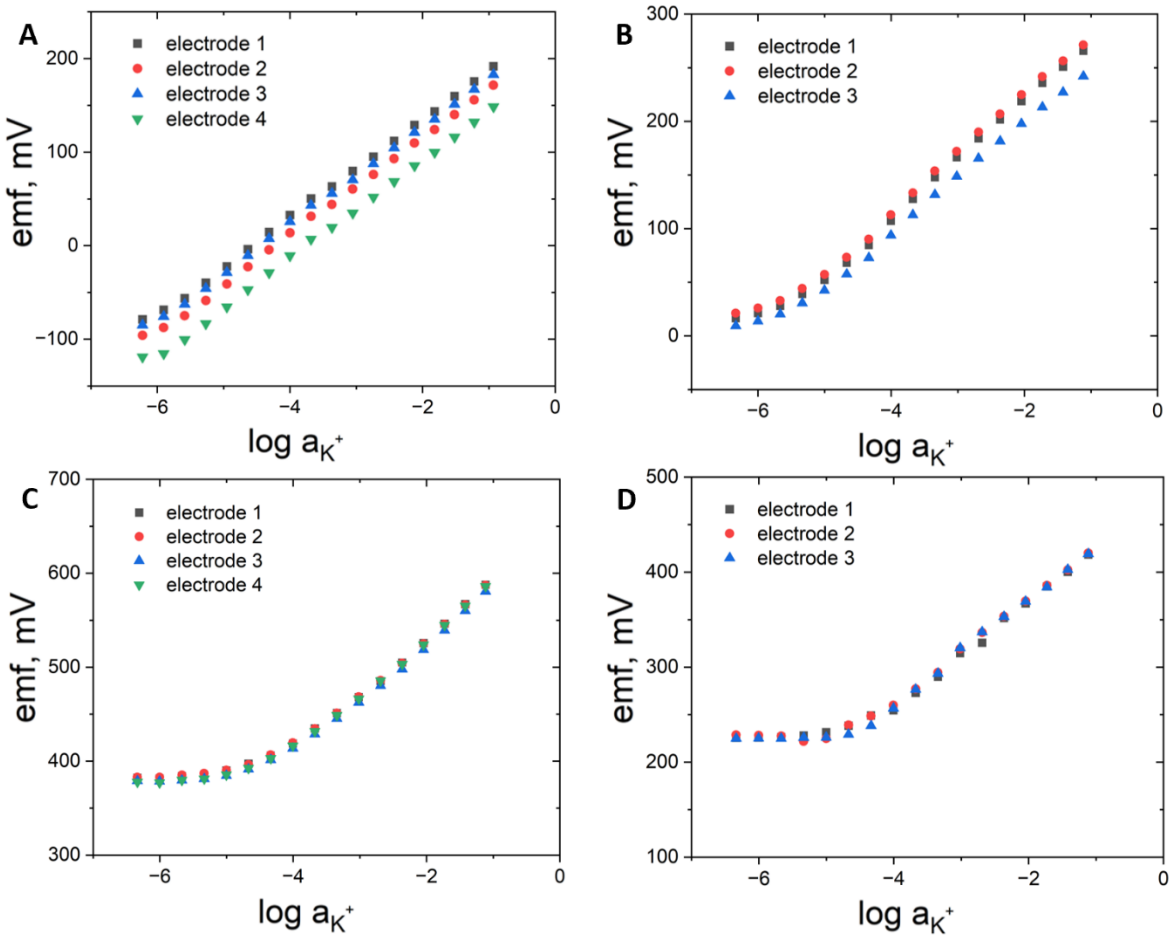


**Figure 3.** Potentiometric $K^+$ response curves of Dow 3140 SC-ISEs with different electrode types, namely (A) graphite/ISM, (B) graphite/CIM carbon/ISM, and (C) graphite/CIM-ph-Tpy-Co(III/II)-Tpy/ISM. For comparison, (D) plasticized PVC SC-ISEs with CIM-ph-Tpy-Co(III/II)-Tpy.

**Table 1.** Potentiometric $K^+$ response values of SC-ISEs with different electrode types.

| electrode type | graphite/CIM carbon with redox buffer/ISM [a] | graphite/CIM carbon/ISM [a] | graphite/ISM [a] | glassy carbon/CIM carbon with redox buffer/ISM [b] |
|---|---|---|---|---|
| $E^o$ (mV)[c] | 645 (± 3.5) | 348 (± 11.5) | 210 (± 23.0) | 483 (± 0.3) |
| Slope (mV/decade) | 59.9 (± 0.4) | 57.9 (± 1.2) | 57.6 (± 0.7) | 56.8 (± 0.4) |

[a] Dow 3140 as membrane matrix. [b] Plasticized PVC as membrane matrix. [c] The $E°$ value represents the potential of the ISE cell obtained by extrapolating the linear portion of the emf response to 1.0 M $K^+$.

As shown in Figure 3, $E°$ reproducibility (that is, the standard deviation of $E°$) was significantly different for the three electrode types. In the absence of a CIM carbon solid contact, the graphite/ISM electrode does not have a well-defined interfacial potential, which resulted in a large $E°$ standard deviation of 23 mV (Figure 3A). When non-functionalized CIM carbon was included as a solid contact, electrodes showed an improved $E°$ reproducibility of 11.5 mV (Figure 3B). This was further reduced to an $E^\circ$ standard deviation of 3.5 mV by use of the CIM carbon functionalized with the attached redox buffer (Figure 3C). Moreover, the electrode potential of ISEs with a Co(III/II) redox buffer solid contact lies approximately half way between those of ISEs with a solid contact modified with either only Co(II) or Co(III) complexes. This, along with a markedly improved electrode reproducibility, confirms the successful oxidation of the Co(III/II) complex with the ferrocenium tetrakis(3-chlorophenyl)borate reagent (see Figure S6 in the Supporting Information). This shows that the Co(III/II) redox buffer was effective in defining the phase boundary potential at the interface of the CIM carbon and the sensing membrane. Based on the amount of the redox buffer in the modified CIM carbon, the redox capacitance at the current peak of the redox couple was calculated to be 3.26 F/g.

According to the newest U.S. Code of Federal Regulations, the maximum acceptable measuring error for $K^+$ detection in clinical laboratories is ± 0.3 mM.[53] In the normal $K^+$

concentration range in human blood of 3.5–5.5 mM,[54] this corresponds to an $E°$ difference of approximately 1.7 mV. This value is smaller than the standard deviation of $E°$ of ± 3.5 mV for the SC-ISEs with the CIM-ph-Tpy-Co(III/II)-Tpy solid contact and the Dow 3140 silicone. Therefore, we wondered whether any improvement in the redox buffer design could improve the $E°$ reproducibility, or whether factors unrelated to the redox buffer had a larger impact on the $E°$ reproducibility.

In order to investigate this, the performance of ISEs with cobalt redox buffer functionalized CIM carbon solid contacts and plasticized PVC sensing membranes were measured too (Figure 3D). Interestingly, ISEs comprising Co(III/II) redox buffer and plasticized PVC as membrane matrix exhibited a very low standard deviation for $E°$ of ± 0.3 mV ($n$ = 3). This indicates that the cause for the lower reproducibility of $E°$ for the SC-ISEs with CIM carbon solid contacts, surface-bound redox buffer, and Dow 3140 silicone membranes is related to the silicone membrane matrix.

We note that Figures 3A and 3B exhibit a detection limit that is lower than what is often observed for $K^+$ ISEs and, in particular, what is shown in Figures 3C and 3D for the ISEs with the Co(III/II) CIM carbon solid contacts. The slightly super-Nernstian response near the detection limit, as it can be seen in Figures 3A and 3B, suggests the presence of an ion flux from the sample into the ISM, possibly caused by the use of the graphite rod. In real-life applications, there is only limited interest in $K^+$ sensing at the low micromolar level, but it will be interesting to observe in future work with ionophores for other target ions whether this observation is limited to $K^+$ or not.

To assess the stability of $E°$ under ambient conditions, the effects of $O_2$ and $CO_2$ were investigated. For this purpose, CIM-ph-Tpy-Co(III/II)-Tpy-based SC-ISEs were immersed in a 1.0 mM KCl solution, and potentiometric measurements were performed while bubbling these gases into the sample solution over 30 min, followed by analogous purging with Ar to remove $O_2$. As

illustrated by Figure S7, exposure to $O_2$ or $CO_2$ did not result in any observable potential shifts, consistent with the control of the phase boundary potential at the interface of the membrane and the CIM carbon by the Co(III/II) redox buffer.

**Long Term Stability of CIM-ph-Tpy-Co(III/II)-Tpy-Based SC-ISEs.** In our previous work, when doping a redox buffer into plasticized PVC membrane, emf drifts of the electrodes were measured over 70 h and were as low as 1.3 μV/h.[37] Longer term experiments were not performed because of the leaching of redox buffer out of the membrane to the sample. Now the problem has been successfully solved by covalently attaching the cobalt redox buffer to the CIM carbon solid contact. Therefore, long-term stabilities of the ISEs with cobalt redox buffer functionalized CIM carbon as solid contact and Dow 3140 or plasticized PVC as sensing membrane matrix were measured over 30 days in 1 mM KCl solution at 25 °C. As shown in Figure 4, the electrodes maintained a good reproducibility from electrode to electrode, with ± 5.6 mV for the standard deviation of $E^o$ for Dow 3140 membrane even after 30 days. The initial 100-hour period also demonstrates remarkable reproducibility in the performance of plasticized PVC membrane electrodes, characterized by a minimal variation of ± 2.8 mV between electrodes. However, a discernible reduction in this reproducibility becomes evident as time elapses. This observed decline in reproducibility may be attributed to the setup employed with the plasticized PVC electrodes. In contrast to the effective sealing achieved with silicone membranes and glass electrode bodies, the PVC electrodes utilize an alternate configuration where the solid contact and membrane are mounted onto the electrode surface with cylindrical electrode bodies, with an o-ring in between the electrode body and ISM. Over time, it is plausible that this setup may eventually fail. One solution to prevent this would be to mount the glassy carbon electrodes into a Tygon tube before applying the modified CIM carbon and ISM, as similarly reported previously.[55]

By comparing the drift behavior between the electrodes with the two different polymeric matrixes, it is obvious that Dow 3140 membranes need longer time to stabilize as compared to PVC membranes, which might be caused by impurities of the silicone slowly leaching into the sample or by continued curing of the silicone membrane. Plasticized PVC membranes typically achieve stabilization more quickly. However, over time, it is possible that the covalent binding of the silicone membrane to the glass body provides for a better seal.

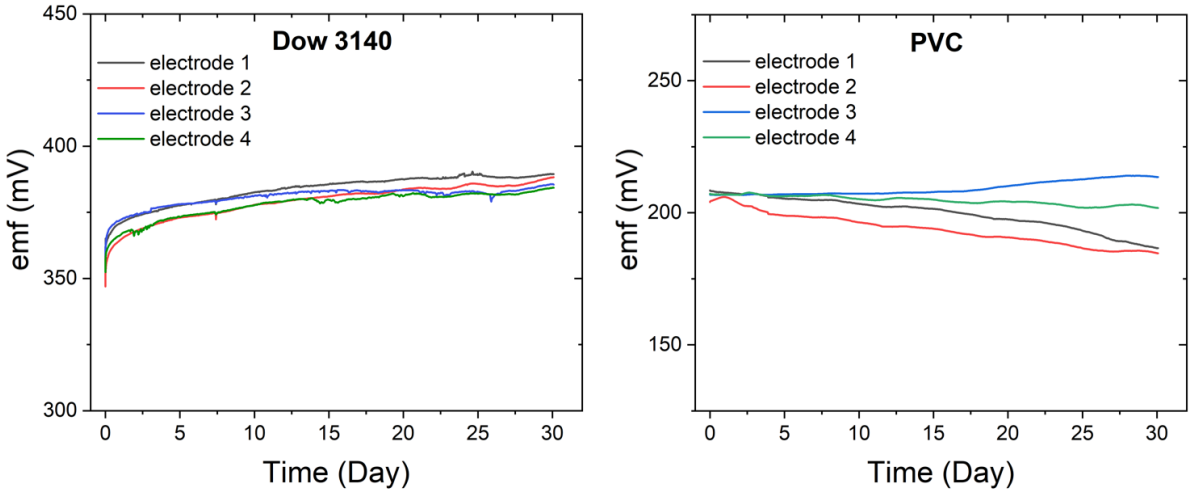


**Figure 4**. Long term stability of the cobalt redox buffer functionalized Dow 3140 SC-ISEs and plasticized PVC SC-ISEs measured over 30 days in 1 mM KCl solution at 25 °C.

## CONCLUSIONS

In this work, a cobalt redox buffer was fabricated using a multi-step process comprising the synthesis of a diazonium derivative of terpyridine (Tpy-ph-$N_2^+$), its covalent attachment to CIM carbon, binding of Co(II) to the surface-attached terpyridine ligands, formation of an octahedral Co(II) complex by reaction with a second terpyridine ligand, and partial oxidation of the surface-attached Co(II) complex to CIM-ph-Tpy-Co(III/II)-Tpy. The CIM carbon functionalized with the cobalt redox buffer was then used as solid-contact material to improve the reproducibility of

electrode potentials in SC-ISEs. By stabilizing the interfacial potential between the solid contact and the ISM, $K^+$-selective SC-ISEs with plasticized PVC ISMs were constructed with a standard deviation of $E°$ as low as 0.3 mV, which suggests the use for calibration-free applications.

When using Dow 3140 silicone as membrane matrix, the $E°$ reproducibility was also enhanced by use of the surface-attached redox buffer, but with a standard deviation of 3.5 mV the improvement was not as pronounced as for the SC-ISEs with plasticized PVC membranes. We conclude that the $E°$ reproducibility is likely not limited by the redox buffer design but by the silicone membrane itself, which may slowly leach impurities into samples or may take very long to completely cure chemically. The benefits of ISEs with silicone membranes became evident though in long-term experiments over 30 days, in which these SC-ISEs exhibited drifts smaller than those observed for electrodes with plasticized PVC membranes.

The advantages of covalently attaching a redox buffer to avoid leaching into sample solutions have been recognized previously by Kozma and co-workers, who prepared a $TEMPO^+/TEMPO^•$ redox buffer in situ by partial electrochemical oxidation.[17, 28] In the current work, partial oxidation of CIM-ph-Tpy-Co(II)-Tpy was performed electroless by use of the new reagent ferrocenium tetrakis(3-chlorophenyl)borate, which may be more amenable to large-scale fabrication of such devices. Long-term potential drift of SC-ISEs with the CIM-ph-Tpy-Co(III/II)-Tpy redox buffer are approximately one order of magnitude smaller than reported drifts[17, 28] for SC-ISEs comprising $TEMPO^+/TEMPO^•$, but further studies will be required to clarify whether this can be explained by the inherent nature of the two redox buffer systems or whether that was caused by other differences in electrode design and characterization.

**ORCID**

Minog Kim: 0000-0001-7963-1734

Xin Dong: 0000-0001-9974-2060

Brian Spindler: 0000-0001-6000-5397

Philippe Bühlmann: 0000-0001-9302-4674

Andreas Stein: 0000-0001-8576-0727

## NOTES

The authors declare the following competing financial interests: A.S., P.B., and the University of Minnesota (UMN) have a patent and a patent application (U.S. patent no. 9,874,539; US2020/059979) relating to the use of CIM carbon in ion-selective and reference electrodes. The UMN and the inventors are entitled to standard royalties should licensing revenue be generated from these inventions.

## ACKNOWLEDGEMENTS

Portions of this work were supported by National Science Foundation Grants CHE-1748148 and 2203752 as well as Medtronic. Parts of this work were carried out at the Characterization Facility, University of Minnesota, which receives partial support from the NSF through the MRSEC (Award Number DMR-2011401) and the NNCI (Award Number ECCS-2025124) programs.

## SUPPORTING INFORMATION

Material characterization, synthesis of CIM carbon, cobalt redox buffer-functionalized CIM carbon, ferrocenium tetrakis(3-chlorophenyl)borate, and cobalt redox buffer-functionalized GCE.

**References**

(1) De Marco, R.; Clarke, G.; Pejcic, B. Ion-Selective Electrode Potentiometry in Environmental Analysis. *Electroanalysis* **2007**, *19* (19-20), 1987-2001.

(2) Bühlmann, P.; Pretsch, E.; Bakker, E. Carrier-Based Ion-Selective Electrodes and Bulk Optodes. 2. Ionophores for Potentiometric and Optical Sensors. *Chem. Rev.* **1998**, *98* (4), 1593-1687.

(3) Crespo, G. A. Recent Advances in Ion-Selective Membrane Electrodes for in Situ Environmental Water Analysis. *Electrochim. Acta* **2017**, *245*, 1023-1034.

(4) Ding, J. W.; Qin, W. Recent Advances in Potentiometric Biosensors. *TrAC, Trends Anal. Chem.* **2020**, *124*, 115803.

(5) Rousseau, C. R.; Bühlmann, P. Calibration-Free Potentiometric Sensing with Solid-Contact Ion-Selective Electrodes. *TrAC, Trends Anal. Chem.* **2021**, *140*, 116277.

(6) Lyu, Y.; Gan, S. Y.; Bao, Y.; Zhong, L. J.; Xu, J. A.; Wang, W.; Liu, Z. B.; Ma, Y. M.; Yang, G. F.; Niu, L. Solid-Contact Ion-Selective Electrodes: Response Mechanisms, Transducer Materials and Wearable Sensors. *Membranes* **2020**, *10* (6), 128.

(7) Cadogan, A.; Gao, Z. Q.; Lewenstam, A.; Ivaska, A.; Diamond, D. All-Solid-State Sodium-Selective Electrode Based on a Calixarene Ionophore in a Poly(Vinyl Chloride) Membrane with a Polypyrrole Solid Contact. *Anal. Chem.* **1992**, *64* (21), 2496-2501.

(8) Bobacka, J. Potential Stability of All-Solid-State Ion-Selective Electrodes Using Conducting Polymers as Ion-to-Electron Transducers. *Anal. Chem.* **1999**, *71* (21), 4932-4937.

(9) Hu, J.; Ho, K. T.; Zou, X. U.; Smyrl, W. H.; Stein, A.; Bühlmann, P. All-Solid-State Reference Electrodes Based on Colloid-Imprinted Mesoporous Carbon and Their Application in Disposable Paper-Based Potentiometric Sensing Devices. *Anal. Chem.* **2015**, *87* (5), 2981-2987.

(10) Hu, J.; Stein, A.; Bühlmann, P. Rational Design of All-Solid-State Ion-Selective Electrodes and Reference Electrodes. *TrAC, Trends Anal. Chem.* **2016**, *76*, 102-114.

(11) Hu, J. B.; Stein, A.; Bühlmann, P. A Disposable Planar Paper-Based Potentiometric Ion-Sensing Platform. *Angew. Chem., Int. Ed. Engl.* **2016**, *55* (26), 7544-7547.

(12) Roy, S.; David-Pur, M.; Hanein, Y. Carbon Nanotube-Based Ion Selective Sensors for Wearable Applications. *ACS Appl. Mater. Interfaces* **2017**, *9* (40), 35169-35177.

(13) Cuartero, M.; Crespo, G. A. All-Solid-State Potentiometric Sensors: A New Wave for in Situ Aquatic Research. *Curr. Opin. Electrochem.* **2018**, *10*, 98-106.

(14) Shao, Y. Z.; Ying, Y. B.; Ping, J. F. Recent Advances in Solid-Contact Ion-Selective Electrodes: Functional Materials, Transduction Mechanisms, and Development Trends. *Chem. Soc. Rev.* **2020**, *49* (13), 4405-4465.

(15) Cheong, Y. H.; Ge, L. Y.; Lisak, G. Highly Reproducible Solid Contact Ion Selective Electrodes: Emerging Opportunities for Potentiometry – a Review. *Anal. Chim. Acta* **2021**, *1162*, 338304.

(16) Zdrachek, E.; Bakker, E. Potentiometric Sensing. *Anal. Chem.* **2021**, *93* (1), 72-102.

(17) Kozmaa, J.; Papp, S.; Gyurcsanyi, R. E. Highly Hydrophobic Tempo-Functionalized Conducting Copolymers for Solid-Contact Ion-Selective Electrodes. *Bioelectrochemistry* **2023**, *150*, 7.

(18) Cattrall, R. W.; Tribuzio, S.; Freiser, H. Potassium-Ion Responsive Coated Wire Electrode Based on Valinomycin. *Anal. Chem.* **1974**, *46* (14), 2223-2224.

(19) Lindner, E.; Gyurcsányi, R. E. Quality Control Criteria for Solid-Contact, Solvent Polymeric Membrane Ion-Selective Electrodes. *J. Solid State Electrochem.* **2009**, *13* (1), 51-68.

(20) Vorotyntsev, M. A.; Heinze, J. Charging Process in Electron Conducting Polymers: Dimerization Model. *Electrochim. Acta* **2001**, *46* (20-21), 3309-3324.

(21) Cheong, Y. H.; Ge, L. Y.; Zhao, N. H.; Teh, L. K.; Lisak, G. Ion Selective Electrodes Utilizing a Ferrocyanide Doped Redox Active Screen-Printed Solid Contact – Impact of Electrode Response to Conditioning. *J. Electroanal. Chem.* **2020**, *870*, 114262.

(22) Fibbioli, M.; Bandyopadhyay, K.; Liu, S. G.; Echegoyen, L.; Enger, O.; Diederich, F.; Gingery, D.; Bühlmann, P.; Persson, H.; Suter, U. W.; Pretsch, E. Redox-Active Self-Assembled Monolayers for Solid-Contact Polymeric Membrane Ion-Selective Electrodes. *J. Mater. Chem.* **2002**, *14* (4), 1721-1729.

(23) Grygolowicz-Pawlak, E.; Wygladacz, K.; Sek, S.; Bilewicz, R.; Brzózka, Z.; Malinowska, E. Studies on Ferrocene Organothiol Monolayer as an Intermediate Phase of Potentiometric Sensors with Gold Inner Contact. *Sens. Actuators, B* **2005**, *111*, 310-316.

(24) Pawlak, M.; Grygolowicz-Pawlak, E.; Bakker, E. Ferrocene Bound Poly(Vinyl Chloride) as Ion to Electron Transducer in Electrochemical Ion Sensors. *Anal. Chem.* **2010**, *82* (16), 6887-6894.

(25) Jaworska, E.; Naitana, M. L.; Stelmach, E.; Pomarico, G.; Wojciechowski, M.; Bulska, E.; Maksymiuk, K.; Paolesse, R.; Michalska, A. Introducing Cobalt(II) Porphyrin/Cobalt(III) Corrole Containing Transducers for Improved Potential Reproducibility and Performance of All-Solid-State Ion-Selective Electrodes. *Anal. Chem.* **2017**, *89* (13), 7107-7114.

(26) Jansod, S.; Wang, L.; Cuartero, M.; Bakker, E. Electrochemical Ion Transfer Mediated by a Lipophilic Os(II)/Os(III) Dinonyl Bipyridyl Probe Incorporated in Thin Film Membranes. *Chem. Commun.* **2017**, *53* (78), 10757-10760.

(27) Jarolímová, Z.; Bosson, J.; Labrador, G. M.; Lacour, J.; Bakker, E. Ion Transfer Voltammetry in Polyurethane Thin Films Based on Functionalised Cationic [6] Helicenes for Carbonate Detection. *Electroanalysis* **2018**, *30* (7), 1378-1385.

(28) Kozma, J.; Papp, S.; Gyurcsányi, R. E. Tempo-Functionalized Carbon Nanotubes for Solid-Contact Ion-Selective Electrodes with Largely Improved Potential Reproducibility and Stability. *Anal. Chem.* **2022**, *94* (23), 8249-8257.

(29) Zou, X. U.; Cheong, J. H.; Taitt, B. J.; Bühlmann, P. Solid Contact Ion-Selective Electrodes with a Well-Controlled Co(II)/Co(III) Redox Buffer Layer. *Anal. Chem.* **2013**, *85* (19), 9350-9355.

(30) Zou, X. U.; Zhen, X. V.; Cheong, J. H.; Bühlmann, P. Calibration-Free Ionophore-Based Ion-Selective Electrodes with a Co(II)/Co(III) Redox Couple-Based Solid Contact. *Anal. Chem.* **2014**, *86* (17), 8687-8692.

(31) Zhen, X. V.; Rousseau, C. R.; Bühlmann, P. Redox Buffer Capacity of Ion-Selective Electrode Solid Contacts Doped with Organometallic Complexes. *Anal. Chem.* **2018**, *90* (18), 11000-11007.

(32) Rousseau, C. R.; Honig, M. L.; Bühlmann, P. Hydrogels Doped with Redox Buffers as Transducers for Ion-Selective Electrodes. *Anal. Chem.* **2022**, *94* (2), 1143-1150.

(33) Lai, C. Z.; Fierke, M. A.; Stein, A.; Bühlmann, P. Ion-Selective Electrodes with Three-Dimensionally Ordered Macroporous Carbon as the Solid Contact. *Anal. Chem.* **2007**, *79* (12), 4621-4626.

(34) Crespo, G. A.; Macho, S.; Rius, F. X. Ion-Selective Electrodes Using Carbon Nanotubes as Ion-to-Electron Transducers. *Anal. Chem.* **2008**, *80* (4), 1316-1322.

(35) Crespo, G. A.; Macho, S.; Bobacka, J.; Rius, F. X. Transduction Mechanism of Carbon Nanotubes in Solid-Contact Ion-Selective Electrodes. *Anal. Chem.* **2009**, *81* (2), 676-681.

(36) Fierke, M. A.; Lai, C. Z.; Bühlmann, P.; Stein, A. Effects of Architecture and Surface Chemistry of Three-Dimensionally Ordered Macroporous Carbon Solid Contacts on Performance of Ion-Selective Electrodes. *Anal. Chem.* **2010**, *82* (2), 680-688.

(37) Hu, J. B.; Zou, X. U.; Bühlmann, P.; Stein, A. Ion-Selective Electrodes with Colloid-Imprinted Mesoporous Carbon as Solid Contact. *Anal. Chem.* **2014**, *86* (14), 7111-7118.

(38) Zdrachek, E.; Bakker, E. Ion-to-Electron Capacitance of Single-Walled Carbon Nanotube Layers before and after Ion-Selective Membrane Deposition. *Microchim. Acta* **2021**, *188* (5), 149.

(39) Dong, X. I. N.; Spindler, B. D.; Kim, M.; Stein, A.; Bühlmann, P. Spontaneous Mesoporosity-Driven Sequestration of Ionic Liquids from Silicone-Based Reference Electrode Membranes. *ACS Sens.* **2023**, *8* (4), 1774-1781.

(40) Morf, W. E. *The Principles of Ion-Selective Electrodes and of Membrane Transport*; Amsterdam : New York, 1981.

(41) Meier, P. C. 2-Parameter Debye-Huckel Approximation for the Evaluation of Mean Activity-Coefficients of 109 Electrolytes. *Anal. Chim. Acta* **1982**, *136*, 363-368.

(42) Hu, J. B.; Zhao, W. Y.; Bühlmann, P.; Stein, A. Paper-Based All-Solid-State Ion-Sensing Platform with a Solid Contact Comprising Colloid-Imprinted Mesoporous Carbon and a Redox Buffer. *ACS Appl. Nano Mater.* **2018**, *1* (1), 293-301.

(43) Phal, S.; Shimizu, K.; Mwanza, D.; Mashazi, P.; Shchukarev, A.; Tesfalidet, S. Electrografting of 4-Carboxybenzenediazonium on Glassy Carbon Electrode: The Effect of Concentration on the Formation of Mono and Multilayers. *Molecules* **2020**, *25* (19), 4575.

(44) Gautier, C.; López, I.; Breton, T. A Post-Functionalization Toolbox for Diazonium (Electro)-Grafted Surfaces: Review of the Coupling Methods. *Mater. Adv.* **2021**, *2* (9), 2773-2810.

(45) Elgrishi, N.; Griveau, S.; Chambers, M. B.; Bedioui, F.; Fontecave, M. Versatile Functionalization of Carbon Electrodes with a Polypyridine Ligand: Metallation and Electrocatalytic $H^+$ and $Co^{2+}$ Reduction. *Chem. Commun.* **2015**, *51* (14), 2995-2998.

(46) Fruehwald, H. M.; Ebralidze, II; Zenkina, O. V.; Easton, E. B. Effect of Transition Metals on the Oxygen Reduction Reaction Activity at Metal-$N_3$/C Active Sites. *Chemelectrochem.* **2021**, *8* (1), 53-61.

(47) Pan, Y. X.; Tong, B.; Shi, J. B.; Zhao, W.; Shen, J. B.; Zhi, J. G.; Dong, Y. P. Fabrication, Characterization, and Optoelectronic Properties of Layer-by-Layer Films Based on Terpyridine-Modified Mwcnts and Ruthenium(III) Ions. *J. Phys. Chem. C* **2010**, *114* (17), 8040-8047.

(48) Cuartero, M.; Bishop, J.; Walker, R.; Acres, R. G.; Bakker, E.; De Marco, R.; Crespo, G. A. Evidence of Double Layer/Capacitive Charging in Carbon Nanomaterial-Based Solid Contact Polymeric Ion-Selective Electrodes. *Chem. Commun.* **2016**, *52* (62), 9703-9706.

(49) Jaworska, E.; Pomarico, G.; Berna, B. B.; Maksymiuk, K.; Paolesse, R.; Michalska, A. All-Solid-State Paper Based Potentiometric Potassium Sensors Containing Cobalt(II) Porphyrin/Cobalt(III) Corrole in the Transducer Layer. *Sens. Actuators, B* **2018**, *277*, 306-311.

(50) Papp, S.; Kozma, J.; Lindfors, T.; Gyurcsányi, R. E. Lipophilic Multi-Walled Carbon Nanotube-Based Solid Contact Potassium Ion-Selective Electrodes with Reproducible Standard Potentials. A Comparative Study. *Electroanalysis* **2020**, *32* (4), 867-873.

(51) Jena, S. R.; Choudhury, J. A Fast-Switching Electrochromic Device with a Surface-Confined 3d Metallo-Organic Coordination Assembly. *Chem. Commun.* **2020**, *56* (4), 559-562.

(52) Bangle, R.; Sampaio, R. N.; Troian-Gautier, L.; Meyer, G. J. Surface Grafting of Ru(II) Diazonium-Based Sensitizers on Metal Oxides Enhances Alkaline Stability for Solar Energy Conversion. *ACS Appl. Mater. Interfaces* **2018**, *10* (3), 3121-3132.

(53) Becerra, X. Clinical Laboratory Improvement Amendments of 1988 (CLIA) Proficiency Testing Regulations Related to Analytes and Acceptable Performance, Federal Register **2022**, *87* (131), 41194-41242.

(54) Rastegar, A. *Serum Potassium in Clinical Methods: The History, Physical, and Laboratory Examinations*; Butterworth, 1990.

(55) Han, T. T.; Kalinichev, A. V.; Mousavi, Z.; Mikhelson, K. N.; Bobacka, J. Anomalous Potentiometric Response of Solid-Contact Ion-Selective Electrodes with Thin-layer Membranes. *Sens. Actuators B* **2022**, *357*, 10, 131416.

## TOC Figure

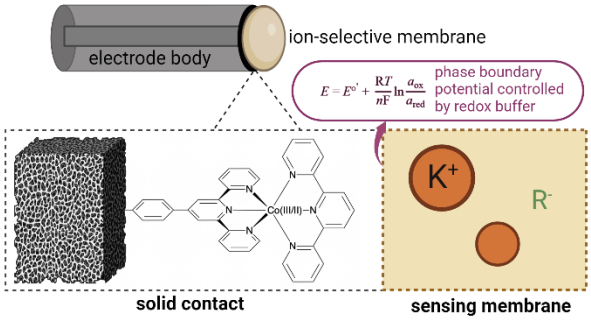
electrode body
ion-selective membrane
$E = E^{o'} + \frac{RT}{nF} \ln \frac{a_{ox}}{a_{red}}$
phase boundary potential controlled by redox buffer
K+
R-
Co(III/II)
solid contact
sensing membrane